Ultrafast time-resolved quantum cascade laser diagnostic for enlightening the role of surface formate species in the photocatalytic oxidation of methanol

Josefine Schnee, Marco Daturi, Mohamad El-Roz

Ultrafast time-resolved quantum cascade laser diagnostic for enlightening the role of surface formate species in the photocatalytic oxidation of methanol

Josefine Schnee,* Marco Daturi, and Mohamad El-Roz,*

Normandie Université, ENSICAEN, UNICAEN, CNRS, Laboratoire Catalyse et Spectrochimie, 14000 Caen, France.

*Corresponding authors. E-mail addresses: josefine.schnee@sorbonne-universite.fr, josischnee@hotmail.com, mohamad.elroz@ensicaen.fr.

Keywords: *Operando* IR; Quantum cascade laser; Photocatalysis; Kinetic constants; Anatase

Abstract

In the present work, a new quantum cascade laser (QCL)-assisted *operando* FT-IR setup was used to get direct insight into the relationship between the overall catalytic performance of TiO_2 photocatalysts in the gas phase photooxidation of methanol at 25 °C, and the kinetics of intermediate surface formate species. Apparent rates of formation ($R_{app,f}$) and reaction ($R_{app,r}$) of surface formates over three different TiO_2 photocatalysts (P25, commercial anatase, and homemade anatase) have been determined through UV on-off cycles under flowing methanol and oxygen. We show that the $R_{app,r}$ follows the same trend as the overall catalytic activity in terms of total yield of methylformate and carbon dioxide, namely the following: TiO_2 P25 ≈ commercial anatase > homemade anatase. So, the faster the reaction of the surface formates is, the higher is the catalytic methanol oxidation activity. Thereby, we demonstrate, to our knowledge for the first time, the direct relationship between the conversion of surface formate species and the catalytic performance of the photocatalysts. Through photocatalytic tests without oxygen in the reaction feed, we also show that the crystallinity of TiO_2 impacts on the availability of its lattice oxygen to contribute for both the formation and conversion of formate species. Indeed, the absence of flowing oxygen reduces the $R_{app,f}$ over TiO_2 CA by a factor 2 while it does not affect that over TiO_2 P25, and it reduces the $R_{app,r}$ over TiO_2 CA about 4 times more than that over TiO_2 P25.

1. Introduction

Photocatalysis is an important and promising approach for green chemistry and sustainable energy solutions.[1,2,3,4] In particular, TiO_2 photochemistry is one of the most important and widely studied approaches for the catalytic conversion of organic compounds,[4,5,6,7] and methanol photochemistry on TiO_2 has often been used as a model reaction to study photocatalytic reaction mechanisms.[1,8,9,10] A powerful tool for such mechanistic investigations is *operando* Fourier-transform infrared (FT-IR) spectroscopy, to unravel surface adsorbed species and reaction intermediates.[11,12,13] The term *operando* means "working/operating" in Latin; and *operando* spectroscopy is a methodology wherein the spectroscopic characterization of materials undergoing reaction is coupled simultaneously with the

measurement of catalytic activity and selectivity (typically by mass spectrometry and/or gas-IR).[14,15] The primary concern of this methodology is to establish structure-activity/selectivity relationships of catalysts in order to gain insight into reaction mechanisms.

In the case of methanol photooxidation over TiO_2, it was previously shown, indirectly through *operando* FT-IR coupled to steady state isotopic exchange kinetic analysis (SSITKA), that the main pathway goes through the chemisorption of methanol as surface methoxy species, then their oxidation into formates and, finally, into CO_2 (with the conversion of chemisorbed formates being the rate-limiting step). In parallel, neighboring adsorbed formates and methoxy groups are supposed to give rise to methylformate, as a secondary species.[1,10] Still, the apparent rate constants of the different reaction steps remained to be determined, and, to our knowledge, there is to date no direct evidence for the key role of formate species in the conversion of methoxy species to CO_2 and methylformate.

To provide this direct evidence is precisely the aim of the present work, in which the apparent rates of formation and reaction of surface formate species on three different TiO_2 photocatalysts (P25, commercial anatase, and homemade anatase) in the gas phase photooxidation of methanol at 25 °C were directly evaluated by using a new quantum cascade laser-assisted *operando* FT-IR setup,[16] and were unprecedentedly correlated with the overall catalytic performance in terms of methanol conversion and selectivity to CO_2 and methylformate. Quantum cascade lasers (QCLs) have been invented in 1994. They are electrically pumped unipolar semiconductor lasers, emitting light through "intersub-band" optical transitions, in contrast to bipolar semiconductor lasers being "interband" lasers. As the photon energy resulting from intersub-band transitions is independent of the band gap of the material in the active region, it can be tuned by adapting the so-called quantum well thickness.[17,18] As described elsewhere,[16] the new setup used in the present work combines a standard FT-IR spectrometer operating in rapid-scan mode (which consists of moving the mobile mirror of the interferometer continuously, and not step by step as in the step-scan mode) with an optical bench containing four QCLs emitting in different (but slightly overlapping) wavenumber ranges within 1876 - 905 cm^{-1}. Within the latter ranges, each of the QCLs is tunable to one single chosen wavenumber. Thanks to an appropriate arrangement of the mirrors, the spectrometer is able to easily switch from the full standard rapid-scan FT-IR to a QCL-irradiation mode tuned to one of the wavenumbers of interest. This is typically of interest when wishing to measure the evolution of one single species – namely formate species in the present work – among others within an interesting spectral region which contains several molecular/structural fingerprints. The rapid-scan mode can provide spectral evidences of the reaction species (on the catalyst or, alternatively, in the gas phase) at the ms time resolution. The QCL-irradiation mode can then be used to follow the IR absorbance of the most relevant species *versus* time with a time resolution of a few microseconds only, which is not achievable with rapid-scan FT-IR, namely depending only on the response time of the detector (here 50 MHz), the QCL pulse rate (settable up to 1 MHz), and the data acquisition system (able to operate with a best time resolution of 3 μs).

The results of the present work demonstrate, to our knowledge for the first time, that the catalytic performance of the photocatalysts directly relies on the conversion rate of the formate species at their

surface. Furthermore, by comparing the apparent rates determined in the absence *vs.* presence of oxygen in the reaction feed, the crystalline nature of the TiO_2 photocatalyst was enlightened to be a key parameter dictating the reactivity of TiO_2 lattice oxygen towards methanol.

2. Experimental section

1. TiO_2 photocatalysts

TiO_2 P25 and commercial anatase (CA hereafter) were purchased from Evonik-Degussa and Sigma-Aldrich, respectively. Homemade anatase (HA hereafter) was prepared as follows. 25 mL of precursor (titanium isopropoxide, TTIP) were introduced into a polypropylene bottle, followed by 9 mL of hydrofluoric acid (40% in water) and 10 mL of acetic acid (stabilizing agents), which were added dropwise while stirring for 30 minutes with a magnetic agitator. The mixture was transferred afterwards to a Teflon reactor, sealed in a stainless-steel autoclave, and then placed into an oven at 200 °C. After 12h of crystallization, the solid recovered in the form of a cloudy mixture was washed with distilled water and ethanol until reaching a neutral pH. The suspended sample was then filtrated, dried at 80 °C for 6h, and finally calcined at 550 °C for 2h (6°C/min).

To evaluate their specific surface area, all three samples were analyzed through nitrogen physisorption at – 196 °C with a Micrometrics Model ASAP 2020 volumetric adsorption analyzer. The samples were outgassed at 250 °C overnight before analysis. The specific surface area was determined from the Brunauer–Emmet–Teller (BET) equation.

2. IR monitoring and photocatalytic testing

The TiO_2 powders were pressed into self-supported discs, all with a similar surface and thickness (2 cm^2 area; 10 mg cm^{-2}; ≈ 65 μm). The resulting pellets were placed into a "Sandwich" transmission IR reactor-cell equipped with KBr windows at each side of the sample holder and with a heating system, and positioned in the sample compartment of the IR spectrometer (Thermo Scientific Nicolet iS50). The IR reactor-cell, described in more details elsewhere,[19] was connected to a gas distribution system equipped with mass flow controllers to introduce gases into the lines (heated at 100 °C). On the other side, to analyze the composition of the outlet gas flow, the reactor-cell was connected to an auxiliary bench of the IR spectrometer equipped with a gas microcell. So, the setup allowed simultaneously IR-observing the surface of the working catalyst pellet and evaluating its catalytic performance, i.e., it allowed *operando* IR characterization.

The IR spectrometer was equipped with a 50 MHz mercury cadmium telluride (MCT) cryo-detector suitable for both standard FT-IR analysis and QCL-time-resolved absorbance diagnostic. As described in more details in reference[16], the spectrometer was coupled with a MIRcat-QT system (Daylight Solutions Inc., San Diego, USA) incorporated into a Thermo Scientific iS50 Research Module, and containing four QCLs. The latter had respectively a spectral tuning range from 1876.2 to

1675.0 cm^{-1}, 1736.1 to 1310.6 cm^{-1}, 1459.9 to 1175.1 cm^{-1} and 1225.5 to 905.0 cm^{-1}. The associated spot size and wavelength accuracy were respectively < 2.5 mm and ≤ 1 cm^{-1}. The linewidth was ≤ 1 cm^{-1} (FWHM). The laser beams were directed to the sample compartment of the spectrometer through the latter but without crossing the interferometer. They were pulsed instead of continuous, in order to avoid local sample heating. The data acquisition system for the QCL mode was provided by STYREL Technologies, partner of National Instruments (NI). It consisted of a NI PXIe-1073 chassis and a PXIe-5122 high resolution oscilloscope card (100 MHz bandwidth) controlled through a PCIe interface integrated within a Ci5 mini-PC configuration, as well as of a custom-made LabVIEW application. The LabVIEW application was designed in such a way that the data acquisition was triggered at each laser pulse (width of 300 ns here). So, in all experiments described in the present work, the time resolution corresponded to the time in-between two successive laser pulses (100 µs here, by setting the pulse rate at 10000 Hz). For each pulse, the amplitude (= maximum – minimum) of the recorded signal curve was automatically exported to a text file *vs.* time, to finally get a curve of amplitude as a function of time consisting of one value every 100 µs. In the standard FT-IR mode (thus with the standard IR source on instead of the QCLs), spectra were collected through the Thermo Scientific OMNIC software, with a spectral resolution of 4 cm^{-1} and 64 scans/spectrum.

Photocatalytic tests of the TiO_2 pellets were performed at 25 °C and atmospheric pressure, under a continuous 30 mL/min reaction flow containing 0.1 vol.% of methanol (Sigma-Aldrich – anhydrous, 99.8%) and 20 vol.% of oxygen carried in argon (continuous flow and high excess of oxygen to minimize the influence of the gas concentrations). The partial pressure of methanol was established using a saturator. As explained in reference[20], UV irradiation of the pellets was carried out with a Xe-Hg lamp (LC8 spot light Hamamatsu, L10852, 200 W), by using a UV-light guide (A10014-50-0110) mounted at the entrance of the IR reactor-cell and flashing the full surface of the wafer. It was verified that the catalyst is homogeneously illuminated and it behaves as a true photo-reactor.

IR monitoring of formate species upon photocatalytic reaction was done in a first series of experiments, with the polychromatic UV light. In a typical experiment, the TiO_2 pellet was first dehydrated by exposure to the reaction flow at 25 °C (to replace water by methanol) without UV irradiation. FT-IR spectra were measured continuously until complete disappearance of the band at 1630 cm^{-1} characteristic[21] of H_2O bending vibrations. At this stage, the UV lamp was already on, but the shutter in-between the lamp and the UV-light guide directed to the IR cell was closed. Then, the photocatalytic test was launched by 1) turning the IR source of the spectrometer and the QCL tuned to the desired wavenumber respectively off and on, and 2) starting the QCL data acquisition system synchronized with the UV shutter in such a way that the shutter opened after 5 s of QCL data acquisition. So, the initial QCL amplitude was measured during 5 s, and then the photocatalytic reaction was launched by enabling UV irradiation of the pellet (already under reaction flow since the dehydration pre-treatment). Depending on the experiments, the shutter remained open for 300 ms or 5 s, after which it was automatically closed again, still under QCL data acquisition to monitor the evolution of remaining adsorbed species once UV irradiation was off. The irradiation on-off cycles were repeated successively three times in each experiment to check the repeatability. At the end, the

QCL was turned off again, and a standard FT-IR spectrum was measured in order to get a full picture of the photocatalyst surface after reaction. As blank tests, three additional experiments were also performed following the same procedure as described above but in the absence of one component per experiment during the whole period of QCL monitoring, namely the component 1) methanol, 2) oxygen, and 3) UV irradiation.

The catalytic activity of the photocatalysts – in terms of methanol conversion and selectivities/yields to/of formaldehyde, methylformate and carbon dioxide – was evaluated in a second step over fresh pellets. The latter were first dehydrated at 25 °C under irradiation with the polychromatic UV light, and then exposed to the reaction flow under irradiation at 365 nm (thanks to a monochromatic 365 nm band pass filter, $I_{0\ (365nm)} \approx 15$ mW/cm²). Using the latter filter aimed at keeping the methanol conversion low enough to enable a proper comparison of the different samples.

3. Results and Discussion

Figure 1 shows the *operando* IR spectra at steady state of TiO_2 P25, CA and HA upon photooxidation of methanol at 25 °C and atmospheric pressure (under a reaction flow of 30 mL/min containing 0.1 vol.% of methanol and 20 vol.% of oxygen in argon). The spectra are shown after subtraction of the initial spectrum recorded after dehydration pre-treatment under the reaction flow (to replace water by methanol), before UV irradiation. The same spectra over a wider range of wavenumbers (4000 to 1000 cm^{-1}) are provided in Figure S1 in the Supplementary Information. The corresponding photocatalytic activities (discussed later) are given in Table 1. Besides the bands in the region from 1050 to 1300 cm^{-1} associated with adsorbed methanol, among which the band at around 1120 cm^{-1} is assigned to the ν(CO) mode of the methoxy species linearly adsorbed on the TiO_2 surface (not further discussed here),[1] the spectra on Figure 1 show bands at 1360, 1380, 1564 and 1580 cm^{-1} associated with ν_s(O–C–O), δ(C–H), ν_{as}(O–C–O)' and ν_{as}(O–C–O) vibrations of surface formate species, respectively.[20,22,23] The ν_{as}(O–C–O)' vibrations are those of formate species bonded to O vacancies in the TiO_2 lattice (so sharing one formate O atom with the TiO_2 surface structure) instead of Ti atoms.[23] As shown by Figures S2 and S3 in the Supplementary Information, the four bands associated with formate species appear neither under UV irradiation alone (without methanol in the flow), nor under reaction flow alone (without UV irradiation). They thus result from the photocatalytic reaction of methanol.

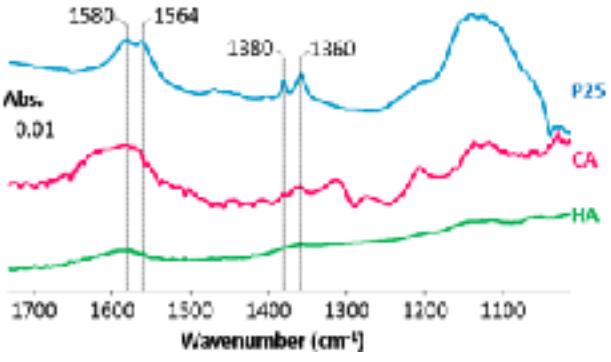

Figure 1. *Operando* FT-IR spectra at steady state of TiO_2 P25, TiO_2 CA and TiO_2 HA upon photooxidation of methanol at 25 °C and atmospheric pressure, shown after subtraction of the initial spectrum recorded after dehydration pre-treatment under flowing methanol before UV irradiation. Conditions: flow = 30 mL/min; 0.1 and 20 vol.% of methanol and oxygen in argon, respectively; Hg-Xe lamp (200 W) filtered at λ = 365 nm; $I_{0\,(365nm)} \approx 15$ mW/cm². "Abs." means absorbance, and is expressed in arbitrary units.

Based on these results (Figure 1), the kinetic behavior (apparent rates) of the surface formate species was monitored by following the intensity of their characteristic IR bands through µs time-resolved QCL diagnostic under transient conditions. More precisely, each of the three TiO_2 samples was submitted to several photocatalytic tests consisting each of three successive UV on-off cycles under reaction flow (30 mL/min, with 0.1 vol.% of methanol and 20 vol.% of oxygen in argon) at 25 °C, and differing from each other by the wavenumber to which the QCL was tuned for monitoring the formation (UV on) and conversion (UV off) of the formate species (at 1360, 1380, 1564 or 1580 cm^{-1}). The formates were always monitored with a QCL pulse rate of 10000 Hz, leading to a time resolution of 100 µs, since it was unnecessary to reach a higher time resolution in this case. The results are shown here only for the mode at 1360 cm^{-1}, the three other wavenumbers showing a similar evolution. For each of the three TiO_2 samples, Figure 2 shows the QCL beam absorbance at 1360 cm^{-1} as a function of time during the first UV on-off cycle (UV on in Figures 2a-b-c, UV off in Figures 2d-e-f). Figures S4 to S8 in the Supplementary Information show the QCL signal at 1360 cm^{-1} *vs.* time over each of the three TiO_2 samples in the whole three repetitions of the UV on-off cycle. From each QCL signal curve, an apparent rate was extracted following the methodology described below for Figure 2. From the three repetitions for each photocatalyst (Figures S4 to S8), the relative error on these apparent rates was estimated to 10%, reflecting a good reproducibility.

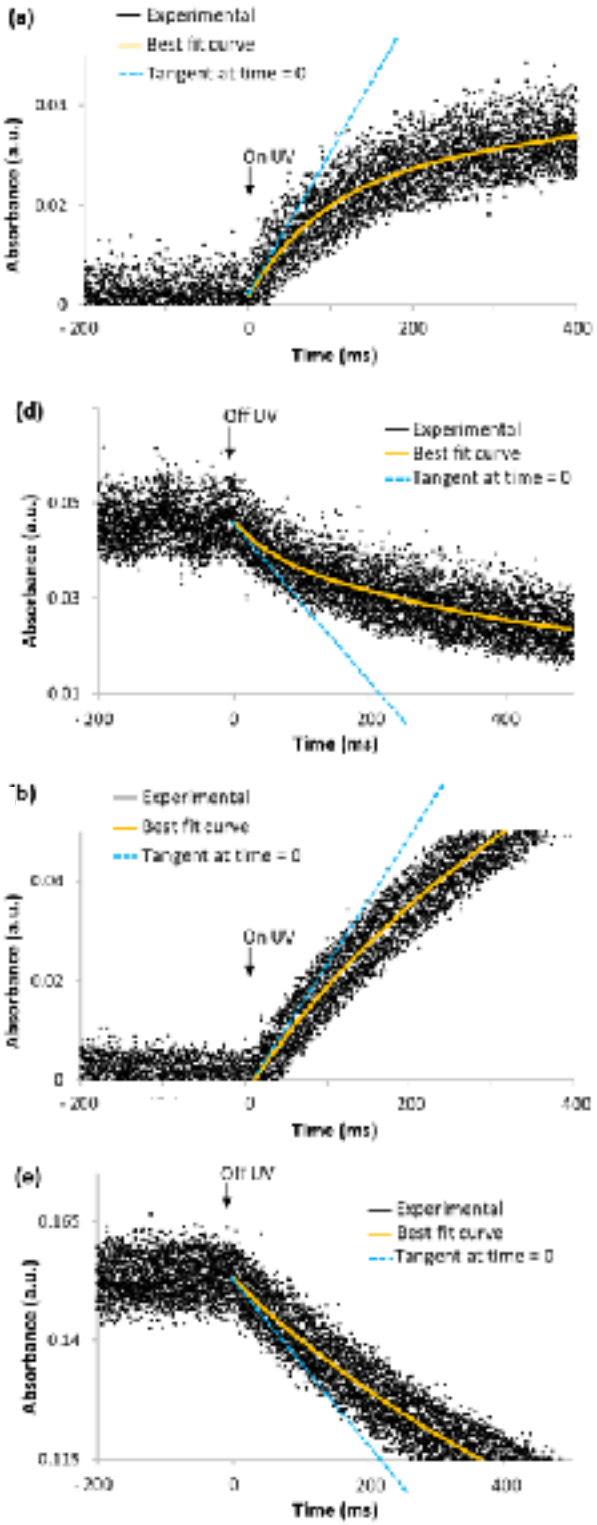
(a)
Experimental
Best fit curve
Tangent at time = 0
On UV
Absorbance (a.u.)
0.01
0.02
0
-200
0
200
400
Time (ms)
(d)
Off UV
Experimental
Best fit curve
Tangent at time = 0
Absorbance (a.u.)
0.03
0.01
-200
0
200
Time (ms)
(b)
Experimental
Best fit curve
Tangent at time = 0
On UV
Absorbance (a.u.)
0.02
0
-200
0
200
400
Time (ms)
(e)
Off UV
Experimental
Best fit curve
Tangent at time = 0
Absorbance (a.u.)
0.14
0.115
-200
0
200
400
Time (ms)

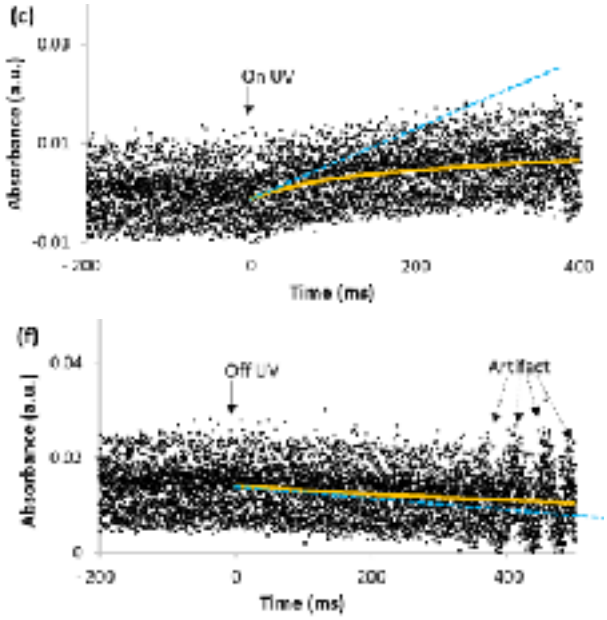

Figure 2. QCL beam absorbance at 1360 cm^{-1} *vs.* time over TiO_2 P25 (a and d), TiO_2 CA (b and e) and TiO_2 HA (c and f) during the first UV on-off cycle (UV on: a-b-c, UV off: d-e-f) under reaction flow at 25 °C and atmospheric pressure. Conditions: flow = 30 mL/min; 0.1 and 20 vol.% of methanol and oxygen in argon, respectively; Hg-Xe lamp (200 W); $I_0 \approx$ 200 mW/cm^2. In (a-b-c), time = 0 corresponds to the moment when the shutter in-between the lamp and the UV-light guide directed to the IR cell was opened to irradiate the sample. During the preceding 200 ms, the sample was already under reaction flow but still in the dark. In (d-e-f), time = 0 corresponds to the moment when the shutter was closed again, still under reaction flow. The fall times to open and to close the shutter were around 6.5 ms and 3.2 ms, respectively, with a minimum pulse width of 13 ms.

On Figures 2a-b-c, the observed QCL absorbance curve (shown again over longer time scales on Figures S4, S6 and S8, respectively) is the result of both the formation and conversion of surface formate species. First, the absorbance increases as a function of time, reflecting that formate species accumulate at the surface of TiO_2. So, in that initial period, the rate of formation is higher than the rate of reaction. Then, after 400 ms to 2.6 s depending on the photocatalyst, steady state is reached. For each photocatalyst, the best fit curve allowed evaluating the initial rate of QCL beam absorption "$(dA/dt)_0$" (slope of the tangent at time = 0, i.e. when the rate of formates consumption tends to zero) directly related to the rate constant "k_f" of formates formation through Equation 1 (with A the QCL beam absorbance due to formate species, ε the integrated molar extinction coefficient at 1360 cm^{-1}, L the optical distance, C_0 the initial concentration of methoxy species getting converted to formates, n the reaction order, and $R_{app,f}$ the apparent rate of formates formation). In fact, working in IR transmission conditions allows taking advantage of the fact that the beam absorbance is proportional to species concentration, so that Equation 1 can be written as a derivation of the Beer-Lambert law. As ε and C_0 are unknown here, direct access to k_f is not provided. So, hereafter, $(dA/dt)_0$ is treated as a whole as an apparent rate "$R_{app,f}$", which is directly related with the rate of formates formation (ε and L in Equation 1 can reasonably be considered constant here from one TiO_2 sample to the next). Therefore, conclusions drawn later in the present work about the parameter "$(dA/dt)_0 = R_{app,f}$" and its relationship with the overall photocatalytic performance (Table 1) are directly applicable to the rate of formates formation.

$$\left(\frac{dA}{dt}\right)_0 = -\varepsilon L\left(\frac{dc}{dt}\right)_0 = \varepsilon L k_f C_0^{\,n} = R_{app,f} \qquad (1)$$

On Figures 2d-e-f, the QCL absorbance decreases with time. Indeed, as UV irradiation is off, the formation of formate species is no longer possible. However, those formate species having accumulated at the surface are converted by an oxidation or crosslinking process with the residual holes or methoxy species, respectively,[1] thereby leading to a progressive decrease of the intensity of the IR band characteristic of formate species. In this case, $(dA/dt)_0$ extracted from the best fit curve is directly related to the rate constant "k_r" of formates reaction through Equation 2 derived from the Beer-Lambert law (with C'_0 the initial concentration of formates remaining at the surface of TiO_2 at the moment when UV irradiation is turned off, m the reaction order, and $R_{app,r}$ the apparent rate of formates reaction). Again, as ε and C'_0 are unknown here, $-(dA/dt)_0$ is treated as a whole as an apparent rate of formates reaction "$R_{app,r}$", which is directly related with the rate of formates reaction (ε and L in Equation 2 can reasonably be considered constant here from one TiO_2 sample to the next). Therefore, conclusions drawn later in the present work about the parameter "$-(dA/dt)_0 = R_{app,r}$" and its relationship with the overall photocatalytic performance (Table 1) are directly applicable to the rate of formates reaction.

$$-\left(\frac{dA}{dt}\right)_0 = -\varepsilon L\left(\frac{dc}{dt}\right)_0 = \varepsilon L k_r C_0^{'\,m} = R_{app,r} \qquad (2)$$

The $R_{app,f}$ and $R_{app,r}$ rates contain three contributions that can change from one TiO_2 photocatalyst to another, and therefore need to be kept in mind for comparing the photocatalytic activities: 1) the intrinsic rate constant of the formation (k_f) and of the conversion (k_r) of surface formate species, 2) the surface coverage of the photocatalyst by the reactants, depending on the concentration of active sites per m² of catalyst (directly impacting on C_0 and C'_0), and 3) the specific surface area of the catalyst (m^2/g) (also directly impacting on C_0 and C'_0).

Table 1 compares the $R_{app,f}$ and $R_{app,r}$ average values over TiO_2 P25, CA and HA, as well as the specific surface areas of the three photocatalysts and their photocatalytic activities. The latter activities (determined from the *operando* IR study) are expressed in terms of methanol conversion, selectivity to formaldehyde (FA), methylformate (MF) and carbon dioxide (CO_2), and total yield of MF+CO_2. The latter total yield is the main parameter to be considered for investigating the relationship between the catalytic activity measured at the outlet of the reactor and the kinetics of formates formation-conversion occurring at the surface of the photocatalysts. Indeed, in the literature, both MF and CO_2 are supposed to result from the conversion of formate species, in turn resulting from the conversion of methoxy species through formaldehyde as an intermediate.[1]

Table 1. For the three TiO_2 photocatalysts studied in this work: specific surface area (SSA), apparent rates of formation and conversion of formate species - $R_{app,f}$ and $R_{app,r}$, respectively (mean values over the three UV on-off cycles) - under reaction flow at 25 °C and atmospheric pressure, and overall photocatalytic activity in terms of methanol conversion (CH_3OH conv.) and selectivity to formaldehyde (FA), methylformate (MF) and carbon dioxide (CO_2) under the same reaction conditions. Estimated error on the conversion and selectivity values: 5 and 10%, respectively. Estimated error on the $R_{app,f}$ and $R_{app,r}$ values: 10%. Conditions: reaction flow = 30 mL/min containing 0.1 and 20 vol.% of methanol and oxygen in argon, respectively; Hg-Xe lamp (200 W) filtered at $\lambda = 365$ nm; $I_{0\,(365nm)} \approx 15$ mW/cm². "Nd" means not detected.

TiO_2 type	SSA [m²/g]	Formates kinetics			CH_3OH conv.	Selectivity				$(MF+CO_2)$ yield
		$R_{app,f}$ [s^{-1}]	$R_{app,r}$ [s^{-1}]	$R_{app,r}/R_{app,f}$		FA	MF	CO_2	Other	
P25	48	0.30	0.15	0.5	0.51	0.17	0.31	0.55	0.01	0.44
CA	85	0.23	0.13	0.56	0.59	0.10	0.29	0.42	0.19	0.42
HA	19	0.06	0.0091	0.15	0.05	0.17	0.16	0.38	Nd	0.027

As shown by Table 1, TiO_2 P25 has an almost 2 times lower specific surface area than TiO_2 CA (48 *vs.* 85 m²/g, respectively). Nevertheless, it reaches slightly higher $R_{app,r}$ and $R_{app,f}$ average values than TiO_2 CA (0.15 *vs.* 0.13 s^{-1} and 0.30 *vs.* 0.23 s^{-1}, respectively). So, given that the R_{app} values depend on the three parameters described earlier (i.e. intrinsic rate constant, surface coverage, and specific surface area; the two latter impacting on C_0 and C'_0), as compared to TiO_2 CA, TiO_2 P25 must have higher intrinsic rate constants for the formation and reaction of formates, and/or a higher concentration of active sites per m² of its surface (thus a higher surface coverage by the reactants), compensating for its lower specific surface area. In any case, in parallel to its slightly faster formates kinetics, TiO_2 P25 also reaches a slightly higher $(MF+CO_2)$ yield than TiO_2 CA (0.44 *vs.* 0.42, respectively). Regarding TiO_2 HA, it has a 4.5 times lower specific surface area than TiO_2 CA (19 *vs.* 85 m²/g, respectively), a 14 times lower $R_{app,r}$, and a 3.8 times lower $R_{app,f}$ (0.0091 *vs.* 0.13 s^{-1} and 0.06 *vs.* 0.23 s^{-1}, respectively). So, as compared to TiO_2 CA, TiO_2 HA must have a considerably lower intrinsic rate constant for the reaction of formates (with a similar surface coverage and a similar intrinsic rate constant for the formation of formates, as the factors 3.8 and 4.5 for the $R_{app,f}$ and the specific surface area, respectively, are of the same order of magnitude). Again, in parallel to its slower formates kinetics, TiO_2 HA also shows a lower $(MF+CO_2)$ yield than TiO_2 CA, precisely 15 times lower, which agrees with its 14 times lower $R_{app,r}$. So, in both the comparisons "TiO_2 P25 *vs.* TiO_2 CA" and "TiO_2 HA *vs.* TiO_2 CA", the $(MF+CO_2)$ yield appears to be directly correlated with the $R_{app,r}$ value associated with the reaction of formates, as illustrated on Figure 3a. Notice that the conversion of methanol – reflecting the overall activity of the photocatalysts – is linearly correlated with the $R_{app,r}/R_{app,f}$ ratio, as shown on Figure 3b. Despite the difficulty to discuss these results quantitatively based on only three photocatalysts, they demonstrate, to our knowledge for the first time here, that the formation of MF and CO_2 occurs through the conversion of formate species at the surface of the photocatalysts, indeed. More generally, they give a direct proof of the relationship between the intrinsic kinetic behavior of the active sites and the overall catalytic performance of the photocatalyst.

The results reveal another important information: the $R_{app,r}$ is 0.15 to 0.56 times lower than the $R_{app,f}$. This proves that the formates conversion is the limiting step of the reaction, in agreement with our previous observation.[1] To our knowledge, the k_r/k_f (equivalent to $R_{app,r}/R_{app,f}$) is determined here for the first time for a heterogeneous photocatalytic reaction. Regarding the fact that the $R_{app,r}$ increases with the $R_{app,f}$ (Figure 3c), it can be mainly assigned to the charge diffusion. The higher the charge separation is, the higher is the activity of the active sites in the formation and conversion of the intermediates (in other words, the higher are the intrinsic rate constants k_f and k_r of the formation and conversion of the intermediates, here the formate species). In the same context, the fact that the formates kinetics, and thus the photocatalytic activities, are similar for TiO_2 P25 and TiO_2 CA although TiO_2 P25 has a 2 times lower specific surface area, is likely due to a higher charge separation (in other words to higher intrinsic k_r and k_f) in the case of TiO_2 P25, ensured by the interface of rutile/anatase phases, if we assume that the concentration of active sites per m² of catalyst surface is similar for the two samples.[24]

Water is suspected to enable a so-called indirect hole transfer and it has been demonstrated through isotopic substitutions that the water content is influencing the reactions outcome.[25] However, in our case, the reaction was performed in "dry" conditions (after purging the surface via a methanol flow, so that it can be assumed that the only water present on the surface is produced by the reaction). Therefore, the concentration of water is negligible with respect to the largely more concentrated adsorbed methanol, whose affinity with the TiO_2 surface is higher than that of water.[1]

Notice that the $R_{app,r}$ values in Table 1 are independent from the UV irradiation time within the UV on-off cycles. Indeed, as demonstrated for TiO_2 P25, the QCL absorbance curve *versus* time in the UV off period following an UV on period of 300 ms is the same as that in the UV off period following an UV on period of 5 s (Figure S9 in the Supplementary Information, with extracted $R_{app,r}$ values of 0.12 and 0.15 s^{-1}, respectively).

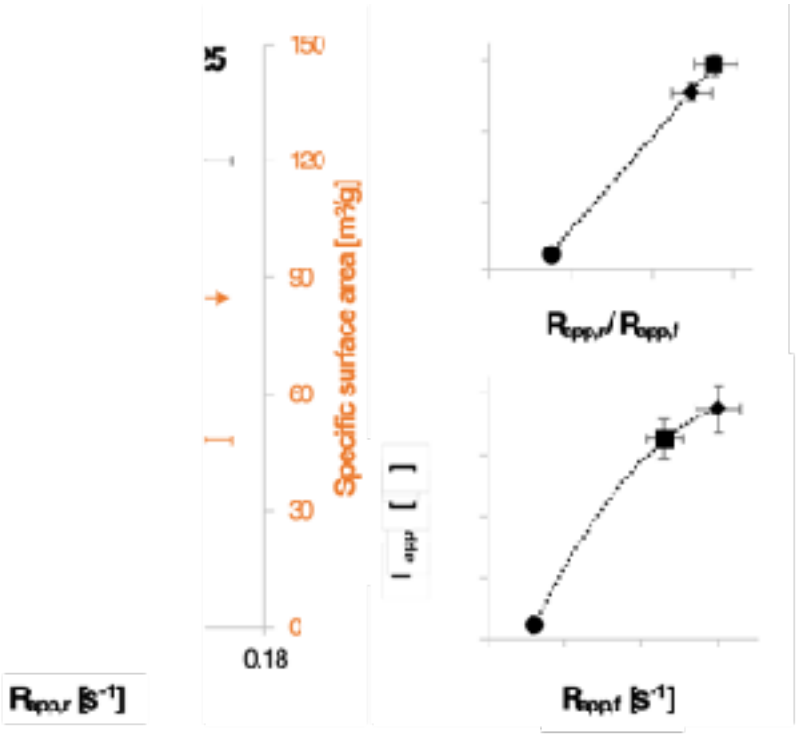

Figure 3. (a) Evolution of the (MF+CO_2) yield *vs.* the $R_{app,r}$ of formate species over TiO_2 HA (circle), CA (square) and P25 (losange) (the specific surface area of the three photocatalysts is also shown, as a reference). (b) Methanol conversion *vs.* $R_{app,r}/R_{app,f}$ ratio of formate species. (c) $R_{app,r}$ *vs.* $R_{app,f}$ of formate species. Conditions: reaction flow = 30 mL/min containing 0.1 and 20 vol.% of methanol and oxygen in argon, respectively; Hg-Xe lamp (200 W) filtered at λ = 365 nm; $I_{0\,(365nm)} \approx 15$ mW/cm^2.

In the case of TiO_2 P25 and CA, the formation-reaction of surface formate species was also monitored in the absence of oxygen in the photocatalytic reaction flow. Figure 4 compares the $R_{app,f}$ and $R_{app,r}$ values of TiO_2 P25 and CA in the absence *vs.* presence of flowing oxygen. These values were extracted as previously from the curves of QCL absorbance at 1360 cm^{-1} *vs.* time, shown here only for TiO_2 P25 on Figure 5. It should be noticed that the conversions were negligible in the absence of oxygen.

In the case of TiO_2 P25, the $R_{app,f}$ is the same in the absence as in the presence of oxygen in the flow (0.3 s^{-1}). This indicates that formate species are able to form with lattice oxygen of TiO_2 as rapidly as with flowing oxygen. However, the $R_{app,r}$ is about three times lower in the absence than in the presence of oxygen in the flow (0.053 *vs.* 0.15 s^{-1}). This reflects that, once formed, the formate species need to react with lattice oxygen coming from the bulk lattice, via complex diffusion pathways, as oxygen from the surface lattice is no longer regenerated by gaseous oxygen, as for example proposed by Ran-ran Feng *et al.*[26] Alternatively, an explanation can be found in the work by Panayotov *et al.*,[5] where it was suggested that under both anaerobic and aerobic conditions, the major oxidation agent is the photogenerated hole, whereas the main role of adsorbed oxygen is to remove the photogenerated electrons by forming superoxide species. As a consequence of electron extraction, the separation of charges would be further improved, leading to a 5-fold increase in formate production, not far from the factor 3 here found. However, it should be noticed that in our case we do not observe superoxides.

The fact that, in the absence of flowing oxygen, the QCL absorbance at 1360 cm^{-1} continues increasing after 400 ms of UV irradiation (Figure 5b) while, in the presence of flowing oxygen, steady state is reached (Figure 5a), is attributed to a raise of baseline due to the accumulation of electrons at the surface of TiO_2 (as those electrons do not meet flowing oxygen to react with).[27] Indeed, as shown on Figure S10 in the Supplementary Information, the QCL absorbance at 1310 cm^{-1}, where no specific absorption band appears here, also increases continuously until the end of the experiment in the absence of oxygen in the flow (whereas in the presence of flowing oxygen it slightly increases only in the first 200 ms before stagnating until the end).

In the case of TiO_2 CA, the absence of flowing oxygen has an even greater impact on $R_{app,r}$, with additionally a significant impact on $R_{app,f}$ (Figure 4). More precisely, $R_{app,r}$ and $R_{app,f}$ are thirteen and two times lower in the absence than in the presence of flowing oxygen, respectively (0.01 *vs.* 0.13 s^{-1}, and 0.11 *vs.* 0.23 s^{-1}). This suggests that lattice oxygen of TiO_2 CA is less available for both the formation and reaction of formates species than lattice oxygen of TiO_2 P25. So, changing the crystallinity of a TiO_2 photocatalyst has an impact on the reactivity of its surface, here towards methanol oxidation.

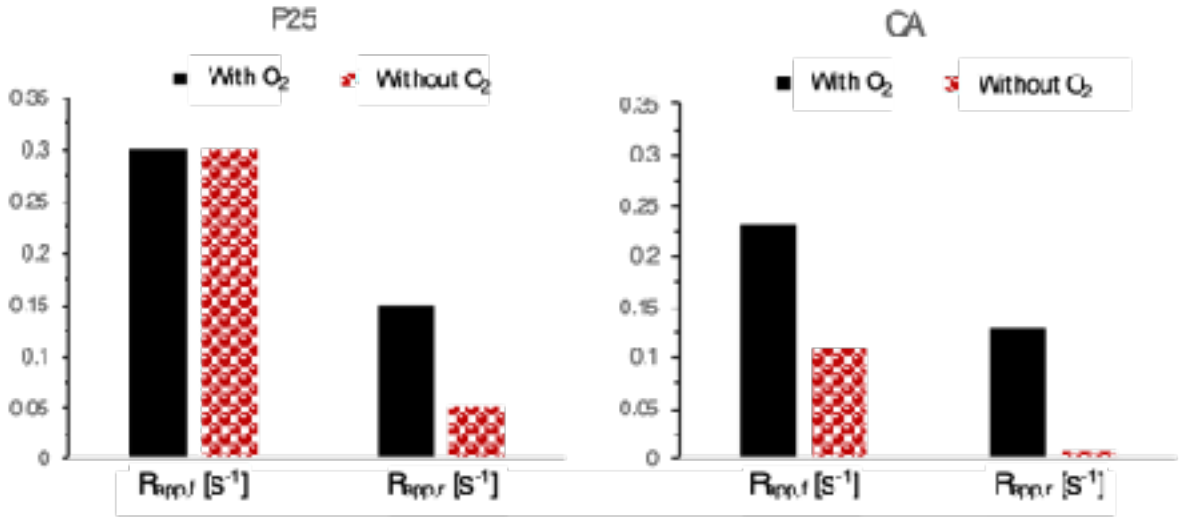

Figure 4. For TiO_2 P25 and CA: apparent rates of formation and reaction of formate species ($R_{app,f}$ and $R_{app,r}$, respectively) at 25 °C and atmospheric pressure in the absence *vs.* presence of oxygen in the reaction flow. Conditions: flow = 30 mL/min; 0.1 vol.% of methanol in argon, with 20 vol.% of oxygen if present; Hg-Xe lamp (200 W); $I_0 \approx 200$ mW/cm^2.

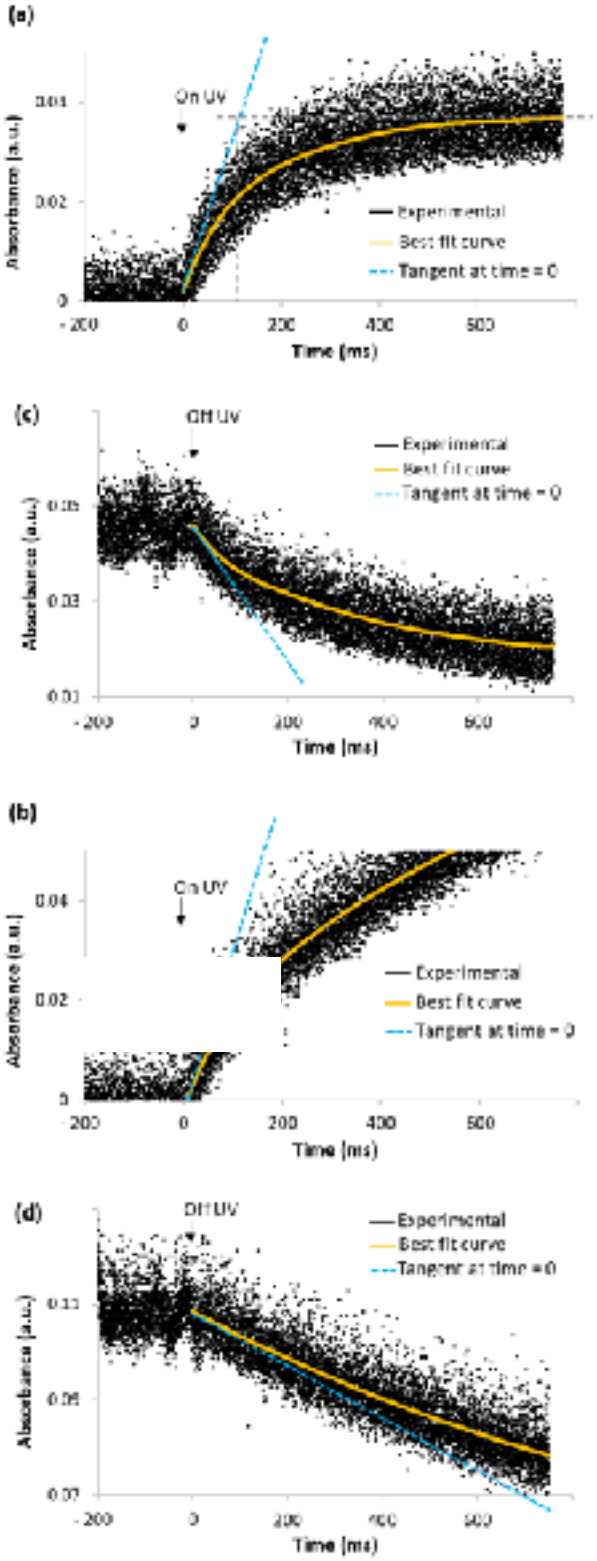

Figure 5. QCL beam absorbance at 1360 cm^{-1} *vs.* time over TiO_2 P25 during a UV on-off cycle (UV on: a-b, UV off: c-d) under flowing methanol at 25 °C and atmospheric pressure in the presence (a and c) or absence (b and d) of oxygen. Conditions: flow = 30 mL/min; 0.1 vol.% of methanol in argon, with 20 vol.% of oxygen if present; Hg-Xe lamp (200 W); I_0 ≈ 200 mW/cm^2. In (a-b), time = 0 corresponds to the moment when the shutter in-between the lamp and the UV-light guide directed to the IR cell was opened to irradiate the sample. During the preceding 200 ms, the sample was already under

flowing methanol (with oxygen in a, without oxygen in b) but still in the dark. In (c-d), time = 0 corresponds to the moment when the shutter was closed again, still under the same flow as in (a-b). The times to open and close the shutter were around 6.5 ms and 3.2 ms, respectively.

4. Conclusions

Three TiO_2 photocatalysts – TiO_2 P25, commercial anatase and homemade anatase – were compared in terms of both photocatalytic activity and formation-conversion kinetics of surface formate species in the photooxidation of methanol at 25 °C and atmospheric pressure. The formates kinetics were monitored with a time resolution of 100 µs, thanks to a QCL tuned to 1360 cm^{-1} (one of the characteristic IR absorption wavenumbers of formates), upon turning UV irradiation on (formates formation) and off (formates conversion) under continuous reaction flow. The photocatalytic activity in terms of total yield of methylformate + carbon dioxide appeared to be directly correlated to the apparent rate of reaction of formates "$R_{app,r}$" (= – the initial rate of QCL beam absorption due to formate species when UV irradiation was turned off). Indeed, both followed the same trend, namely TiO_2 P25 ≈ commercial anatase > homemade anatase. So, the faster the conversion of the surface formates is, the higher is the catalytic methanol oxidation activity. This demonstrates, to our knowledge for the first time, that the formation of methylformate and carbon dioxide occurs through the conversion of formate species at the surface of the photocatalysts, indeed. Furthermore, the conversion of formates was revealed to be the rate-limiting step of the reaction, thanks to k_r/k_f (= intrinsic rate constant of formates conversion/intrinsic rate constant of formates formation) ratios determined here for the first time, to our knowledge. Finally, we also found that the crystallinity of TiO_2 impacts on the availability of its lattice oxygen to contribute for both the formation and reaction of formate species. Indeed, removing oxygen from the reaction flow reduces the $R_{app,f}$ over TiO_2 CA by a factor 2 while it does not affect that over TiO_2 P25, and it reduces the $R_{app,r}$ over TiO_2 CA about 4 times more than that over TiO_2 P25.

Associated content

Supporting Information. FT-IR spectra of TiO_2 P25 before and during UV irradiation with only oxygen in the flow (no methanol) at 25 °C, and plots of the amplitude of the QCL signal *versus* time in various conditions.

Author information

All authors have given approval to the final version of the manuscript.

Present address of Josefine Schnee : Sorbonne Université, CNRS, Laboratoire de Réactivité de Surface (LRS), Tour 43, Case 178, 4, Place Jussieu, F-75252 Paris Cedex 05, France.

Acknowledgements

J. Schnee and M. Daturi acknowledge the LabEx EMC3 and the European Union for the cofunding via the contract “DRUID” and the operational program FEDER/FSE 2014-2020, respectively. The authors acknowledge Yoann Levaque and Oumaima Thili (Laboratoire Catalyse et Spectrochimie, Université de Caen, France) for the technical support and for providing the homemade anatase sample, respectively.

Competing interests

The authors declare no competing interests.

References

1. El-Roz, M.; Bazin, P.; Daturi, M.; Thibault-Starzyk, F., On the mechanism of methanol photooxidation to methylformate and carbon dioxide on TiO_2: an *operando*-FTIR study. *Physical Chemistry Chemical Physics* **2015,** *17* (17), 11277-11283.
2. Yoon, T. P., Visible Light Photocatalysis: The Development of Photocatalytic Radical Ion Cycloadditions. *ACS Catalysis* **2013**, *3* (5), 895-902.
3. Chen, H.; Nanayakkara, C. E.; Grassian, V. H., Titanium Dioxide Photocatalysis in Atmospheric Chemistry. *Chem. Rev.* **2012**, *112* (11), 5919-5948.
4. Schneider, J.; Matsuoka, M. ; Takeuchi, M. ; Zhang, J. ; Horiuchi, Y. ; Anpo, M. ; Bahnemann, D. W., Understanding TiO_2 Photocatalysis: Mechanisms and Materials. *Chem. Rev.* **2014**, *114*, 9919−9986.
5. Panayotov, D.A. ; Burrows, S. P. ; Morris, J. R., Photooxidation Mechanism of Methanol on Rutile TiO_2 Nanoparticles. *J. Phys. Chem. C* **2012**, *116*, 6623−6635.
6. Tamaki, Y. ; Hara, K. ; Katoh, R. ; Tachiya, M. ; Furube, A., Femtosecond Visible-to-IR Spectroscopy of TiO_2 Nanocrystalline Films: Elucidation of the Electron Mobility before Deep Trapping. *J. Phys. Chem. C* **2009**, *113,* 11741–11746.
7. Shen, S. ; Wang, X. ; Chen, T. ; Feng, Z. ; Li, C., Transfer of Photoinduced Electrons in Anatase−Rutile TiO_2 Determined by Time-Resolved Mid-Infrared Spectroscopy. *J. Phys. Chem. C* **2014**, *118*, 12661−12668.
8. Chuang, C-C. ; Chen, C-C. ; Lin, J-L., Photochemistry of Methanol and Methoxy Groups Adsorbed on Powdered TiO_2. *J. Phys. Chem. B* **1999**, *103,* 2439-2444.
9. Wolski, L.; El-Roz, M.; Daturi, M.; Nowaczyk, G.; Ziolek, M., Insight into methanol photooxidation over mono- (Au, Cu) and bimetallic (AuCu) catalysts supported on niobium pentoxide — An *operando*-IR study. *Applied Catalysis B: Environmental **2019**, 258*, 117978.
10. El-Roz, M. ; Bazin, P. ; Daturi, M. ; Thibault-Starzyk, F., *Operando* Infrared (IR) Coupled to Steady-State Isotopic Transient Kinetic Analysis (SSITKA) for Photocatalysis: Reactivity and Mechanistic Studies, *ACS Catal*. **2013**, *3*, 2790−2798.
11. Vimont, A. ; Thibault-Starzyk, F. ; Daturi, M., Analysing and understanding the active site by IR spectroscopy. *Chem. Soc. Rev.,* **2010**, *39*, 4928–4950.

12. Mino, L., IR spectroscopy as a tool to investigate photocatalytic reactions at oxide surfaces. *Rendiconti Lincei* **2017**, *28*, 143–149.
13. Ftouni, K. ; Lakiss, L. ; Thomas, S. ; Daturi, M. ; Fernandez, C. ; Bazin, P. ; El Fallah, J. ; El-Roz, M., TiO_2/Zeolite Bifunctional (Photo)Catalysts for a Selective Conversion of Methanol to Dimethoxymethane : On the Role of Brønsted Acidity. *J. Phys. Chem. C* **2018**, *122*, 29359−29367.
14. Bañares, M. A., *Operando* methodology: combination of in situ spectroscopy and simultaneous activity measurements under catalytic reaction conditions. *Catal. Today* **2005**, *100* (1–2), 71–77.
15. Schnee, J. ; Gaigneaux, E.M., Elucidating and exploiting the chemistry of Keggin heteropolyacids in the methanol-to-DME conversion: enabling the bulk reaction thanks to operando Raman. *Catal. Sci. Technol.* **2017**,*7*, 817-830.
16. Schnee, J.; Bazin, P.; Barviau, B.; Grisch, F.; Beccard, B. J.; Daturi, M., Coupling a Rapid-Scan FT-IR Spectrometer with Quantum Cascade Lasers within a Single Setup: An Easy Way to Reach Microsecond Time Resolution without Losing Spectral Information. *Analytical Chemistry* **2019,** *91* (7), 4368-4373.
17. Waried, H. H., Synchronization of quantum cascade lasers with mutual optoelectronic coupling. *Chinese J. Phys.* **2018,** *56* (3), 1113-1120.
18. Tittel, F. K.; Bakhirkin, Y.; Kosterev, A. A.; Wysocki, G., Recent Advances in Trace Gas Detection Using Quantum and Interband Cascade Lasers. *Rev Laser Eng* **2006,** *34* (4), 275-282.
19. Lesage, T.; Verrier, C.; Bazin, P.; Saussey, J.; Daturi, M., Studying the NO-trap mechanism over a Pt-Rh/Ba/Al_2O_3 catalyst by *operando* FT-IR spectroscopy. *Physical Chemistry Chemical Physics* **2003,** *5* (20), 4435-4440.
20. El-Roz, M.; Bazin, P.; Thibault-Starzyk, F., An operando-IR study of photocatalytic reaction of methanol on new *BEA supported TiO_2 catalyst. *Catalysis Today* **2013,** *205*, 111-119.
21. Frost, R. L., An infrared and Raman spectroscopic study of the uranyl micas. *Spectrochimica Acta Part A: Molecular and Biomolecular Spectroscopy* **2004,** *60* (7), 1469-1480.
22. Groff, R. P.; Manogue, W. H., An infrared study of formate formation and reactivity on TiO_2 surfaces. *Journal of Catalysis* **1983,** *79* (2), 462-465.
23. Andersson, M.; Kiselev, A.; Österlund, L.; Palmqvist, A. E. C., Microemulsion-Mediated Room-Temperature Synthesis of High-Surface-Area Rutile and Its Photocatalytic Performance. *The Journal of Physical Chemistry C* **2007,** *111* (18), 6789-6797.
24. Li, G.; Richter, C. P.; Milot, R. L.; Cai, L.; Schmuttenmaer, C. A.; Crabtree, R. H.; Brudvig, G. W.; Batista, V. S., Synergistic effect between anatase and rutile TiO_2 nanoparticles in dye-sensitized solar cells. *Dalton Transactions* **2009,** (45), 10078-10085.
25. Chiarello, G. L.; Ferri, D.; Selli, E., Effect of the CH_3OH/H_2O ratio on the mechanism of the gas-phase photocatalytic reforming of methanol on noble metal-modified TiO_2. *Journal of Catalysis* **2011,** *280* (2), 168-177.

26. Feng, R.-r.; Liu, A.-a.; Liu, S.; Shi, J.; Zhang, R.; Ren, Z., *In Situ* Studies on the Dissociation and Photocatalytic Reactions of CH_3OH on TiO_2 Thin Film by Sum Frequency Generation Vibrational Spectroscopy. *The Journal of Physical Chemistry C* **2015,** *119* (18), 9798-9804.
27. Guzman, F.; Chuang, S. S. C., Tracing the Reaction Steps Involving Oxygen and IR Observable Species in Ethanol Photocatalytic Oxidation on TiO_2. *Journal of the American Chemical Society* **2010,** *132* (5), 1502-1503.

TOC graphic

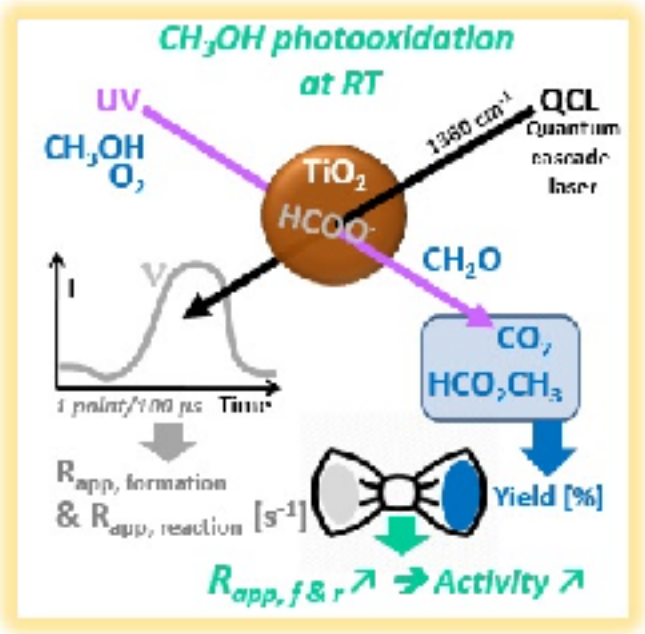

Ultrafast time-resolved quantum cascade laser diagnostic for enlightening the role of surface formate species in the photocatalytic oxidation of methanol

Josefine Schnee,* Marco Daturi, and Mohamad El-Roz,*

Normandie Université, ENSICAEN, UNICAEN, CNRS, Laboratoire Catalyse et Spectrochimie, 14000 Caen, France.

*Corresponding authors. E-mail addresses: josefine.schnee@sorbonne-universite.fr, josischnee@hotmail.com, mohamad.elroz@ensicaen.fr.

Supplementary Information

- **Full *operando* FT-IR spectra at steady state of TiO_2 P25, CA and HA upon photooxidation of methanol at 25 °C and atmospheric pressure (under a reaction flow of 30 mL/min containing 0.1 vol.% of methanol and 20 vol.% of oxygen in argon).**

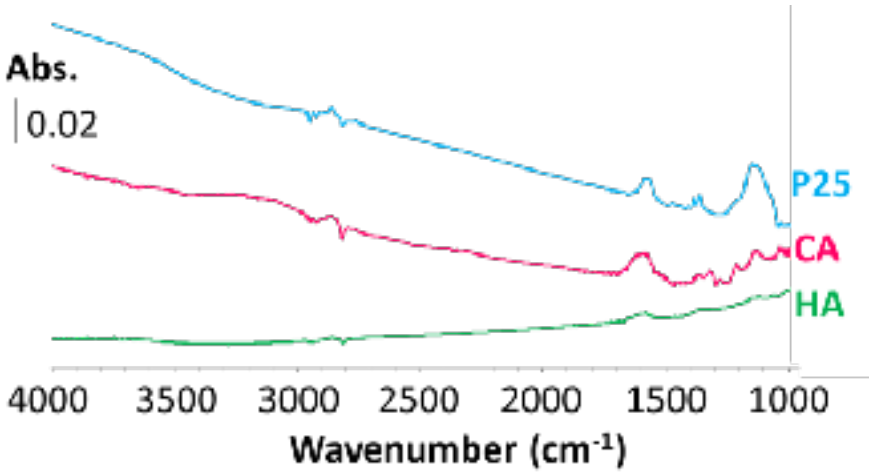

Figure S1. Full *operando* FT-IR spectra at steady state of TiO_2 P25, TiO_2 CA and TiO_2 HA upon photooxidation of methanol at 25 °C and atmospheric pressure, shown after subtraction of the initial spectrum recorded after dehydration pre-treatment under flowing methanol before UV irradiation. Conditions: flow = 30 mL/min; 0.1 and 20 vol.% of methanol and oxygen in argon, respectively; Hg-Xe lamp (200 W) filtered at λ = 365 nm; $I_{0\,(365nm)} \approx 15$ mW/cm^2. "Abs." means absorbance, and is expressed in arbitrary units.

- **FT-IR spectra of TiO_2 P25 before and during UV irradiation at 25 °C under a flow of 20 vol. % oxygen in argon (no methanol).**

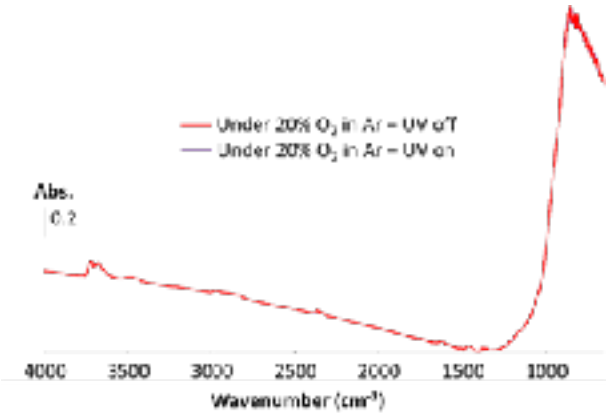

Figure S2. FT-IR spectra of TiO_2 P25 before and during UV irradiation at 25 °C and atmospheric pressure under a flow of 20 vol.% oxygen in argon without methanol. Conditions: flow = 30 mL/min; Hg-Xe lamp (200 W); $I_0 \approx 200$ mW/cm². "Abs." means absorbance, and is expressed in arbitrary units.

- **QCL beam amplitude at 1360 cm^{-1} over TiO_2 P25 at 25 °C under reaction flow (methanol + oxygen/argon) without UV irradiation.**

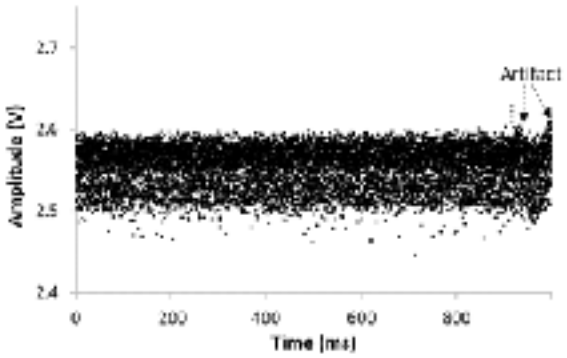

Figure S3. QCL beam amplitude at 1360 cm^{-1} *vs* time over TiO_2 P25 under reaction flow at 25 °C and atmospheric pressure without UV irradiation. Conditions: flow = 30 mL/min; 0.1 and 20 vol.% of methanol and oxygen in argon, respectively.

- **QCL signal at 1360 cm^{-1} *vs* time over TiO_2 P25 in 3 repetitions of the UV on-off cycle under reaction flow at 25 °C.**

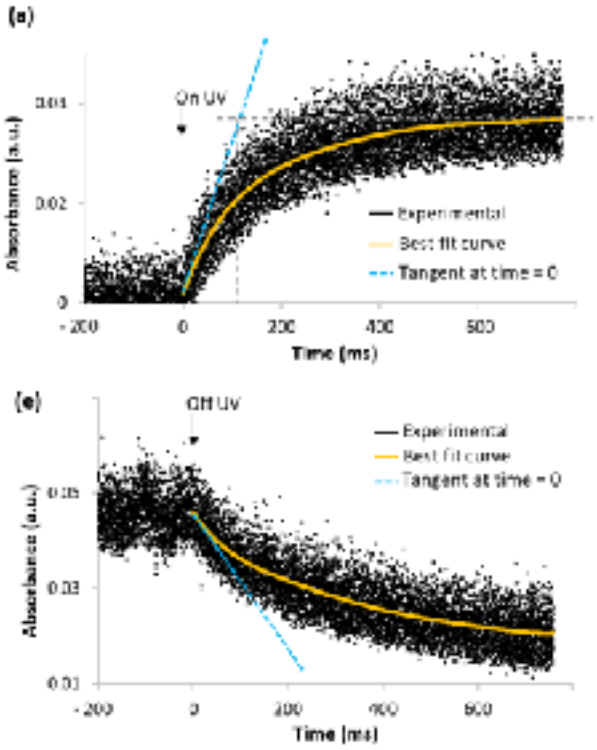

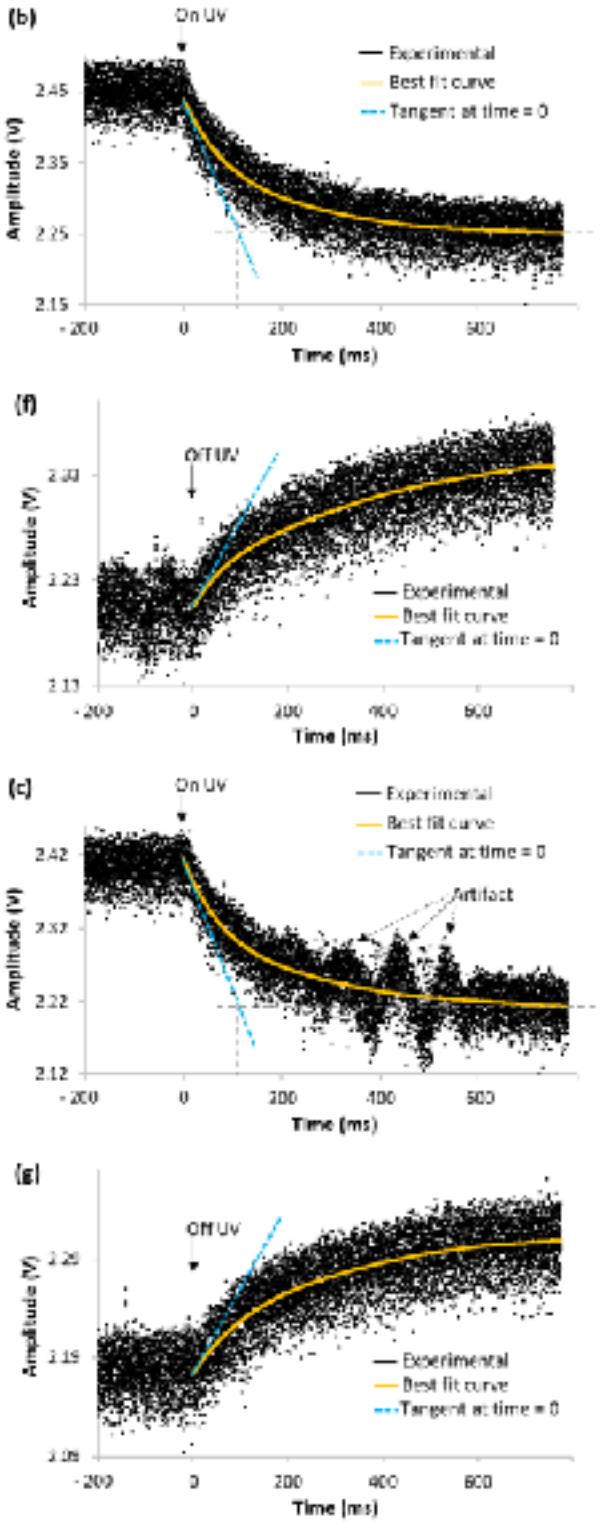
(b)
On UV
Experimental
Best fit curve
Tangent at time = 0
Amplitude (V)
2.45
2.35
2.25
2.15
-200
0
200
400
600
Time (ms)
(f)
Off UV
Amplitude (V)
Experimental
Best fit curve
Tangent at time = 0
Time (ms)
(c)
On UV
Experimental
Best fit curve
Tangent at time = 0
Artifact
Amplitude (V)
2.42
2.32
2.22
2.12
-200
0
200
400
600
Time (ms)
(g)
Off UV
Amplitude (V)
Experimental
Best fit curve
Tangent at time = 0
-200
0
200
400
600
Time (ms)

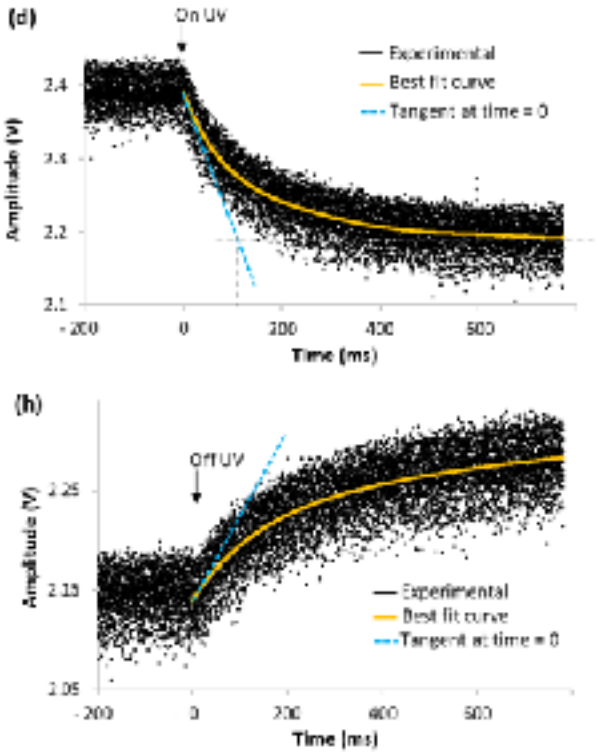

Figure S4. QCL signal at 1360 cm^{-1} *vs* time over TiO_2 P25 during repeated UV on-off cycles (UV on: a-b-c-d, UV off: e-f-g-h; two panels on the same horizontal line forming one UV on-off cycle) under reaction flow at 25 °C and atmospheric pressure. (a) and (e) show the same UV on-off cycle as (b) and (f), but with a y axis expressed in absorbance instead of amplitude. Conditions: flow = 30 mL/min; 0.1 and 20 vol.% of methanol and oxygen in argon, respectively; Hg-Xe lamp (200 W); $I_0 \approx 200$ mW/cm^2. In (a-b-c-d), time = 0 corresponds to the moment when the shutter in-between the lamp and the UV-light guide directed to the IR cell was opened to irradiate the sample. During the preceding 200 ms, the sample was already under reaction flow but still in the dark. In (e-f-g-h), time = 0 corresponds to the moment when the shutter was closed again, still under reaction flow. The times to open and close the shutter were around 6.5 ms and 3.2 ms, respectively.

- **QCL signal at 1360 cm^{-1} *vs* time over TiO_2 CA in 3 repetitions of the UV on-off cycle under reaction flow at 25 °C.**

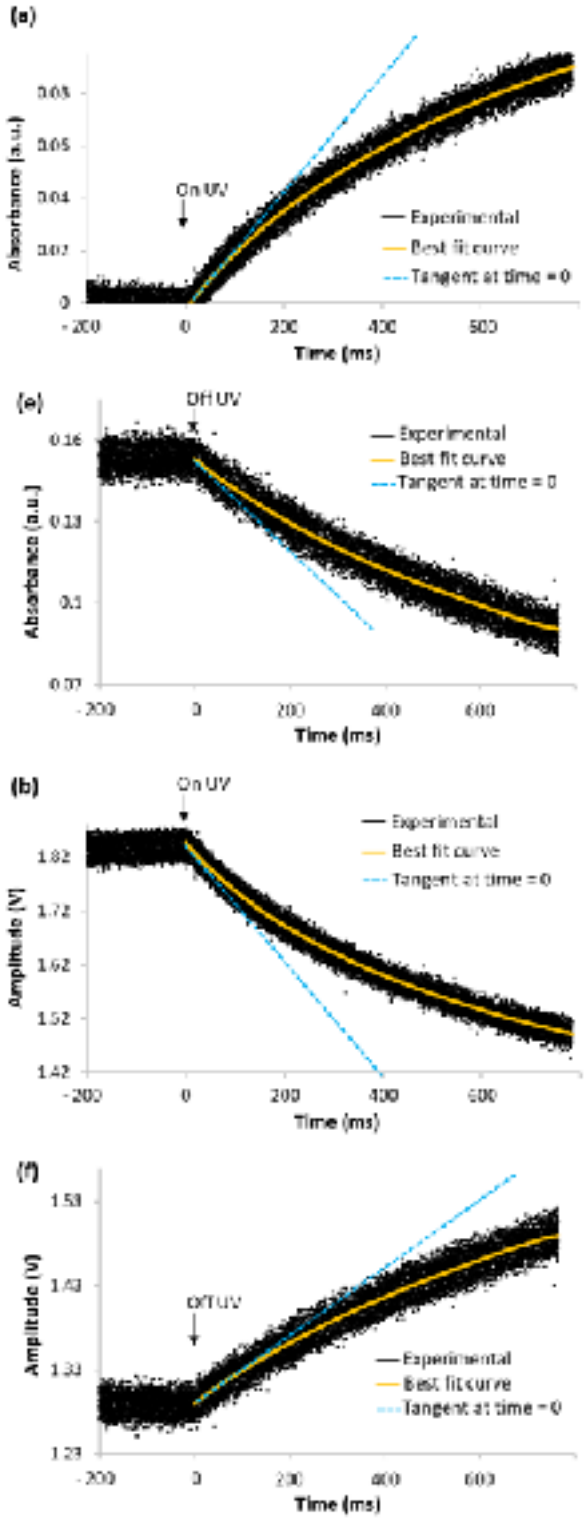
(a)
On UV
Experimental
Best fit curve
Tangent at time = 0
Absorbance (a.u.)
Time (ms)
(e)
Off UV
Experimental
Best fit curve
Tangent at time = 0
Absorbance (a.u.)
Time (ms)
(b)
On UV
Experimental
Best fit curve
Tangent at time = 0
Amplitude (V)
Time (ms)
(f)
Off UV
Experimental
Best fit curve
Tangent at time = 0
Amplitude (V)
Time (ms)

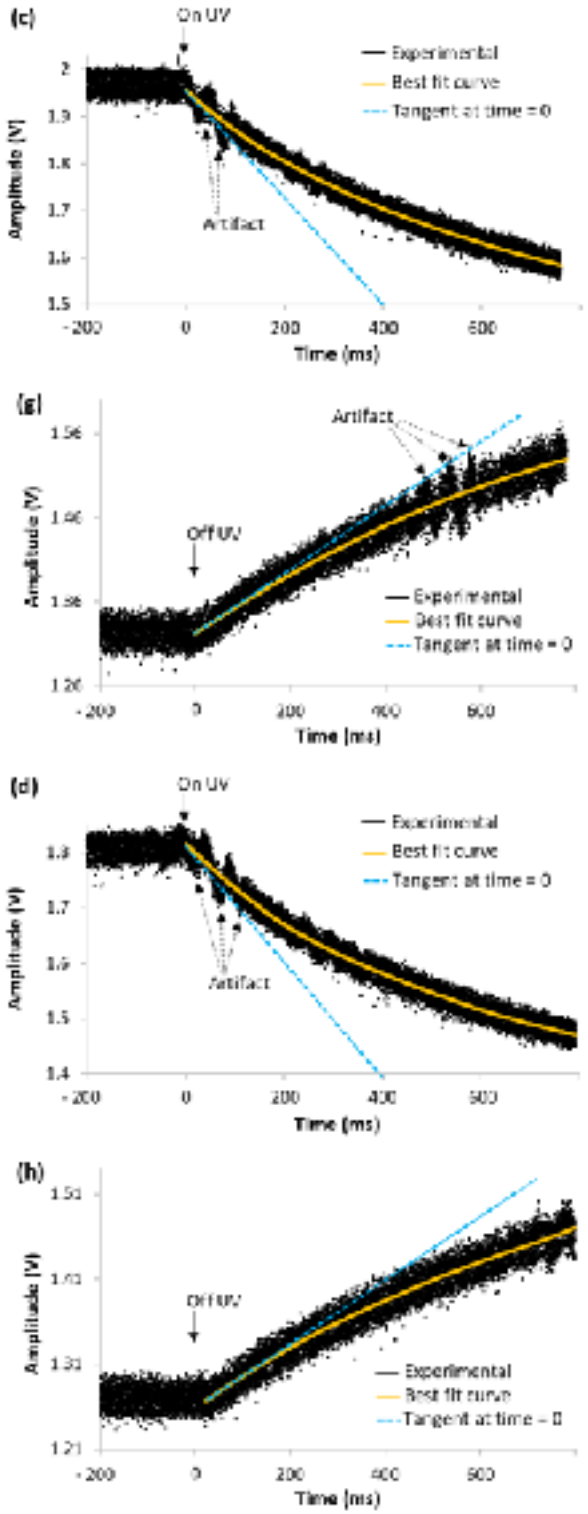

Figure S5. QCL signal at 1360 cm^{-1} *vs* time over TiO_2 CA during repeated UV on-off cycles (UV on: a-b-c-d, UV off: e-f-g-h; two panels on the same horizontal line forming one UV on-off cycle) under reaction flow at 25 °C and atmospheric pressure. (a) and (e) show the same UV on-off cycle as (b) and (f), but with a y axis expressed in absorbance instead of amplitude. Conditions: flow = 30 mL/min; 0.1 and 20 vol.% of methanol and oxygen in argon, respectively; Hg-Xe lamp (200 W); $I_0 \approx 200$ mW/cm^2. In (a-b-c-d), time = 0 corresponds to the moment when the shutter in-between the lamp and the UV-light guide directed to the IR cell was opened to irradiate the sample. During the preceding 200 ms, the sample was already under reaction flow but still in the dark. In (e-f-g-h), time = 0 corresponds to the moment when the shutter was closed again, still under reaction flow. The times to open and close the shutter were around 6.5 ms and 3.2 ms, respectively.

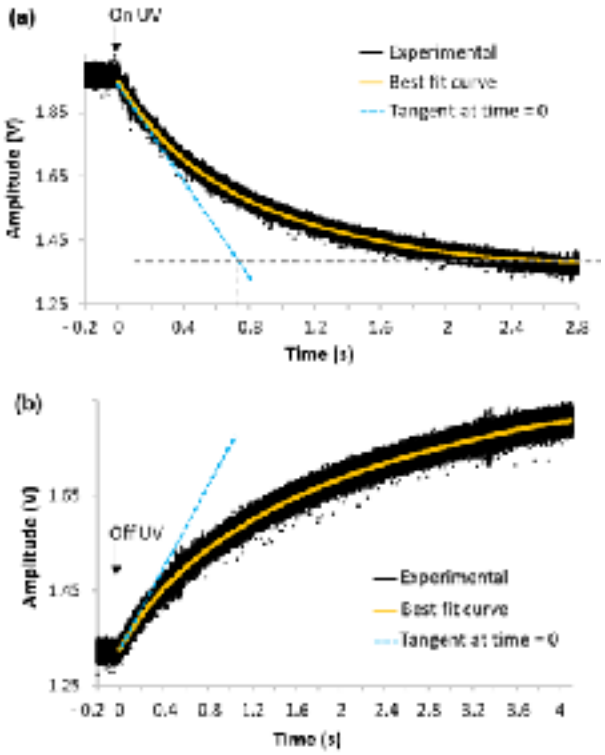

Figure S6. Same UV on(a)-off(b) cycle as shown on Figure S5 (c and g, respectively), but over a longer time scale.

- **QCL signal at 1360 cm^{-1} *vs* time over TiO_2 HA in 3 repetitions of the UV on-off cycle under reaction flow at 25 °C.**

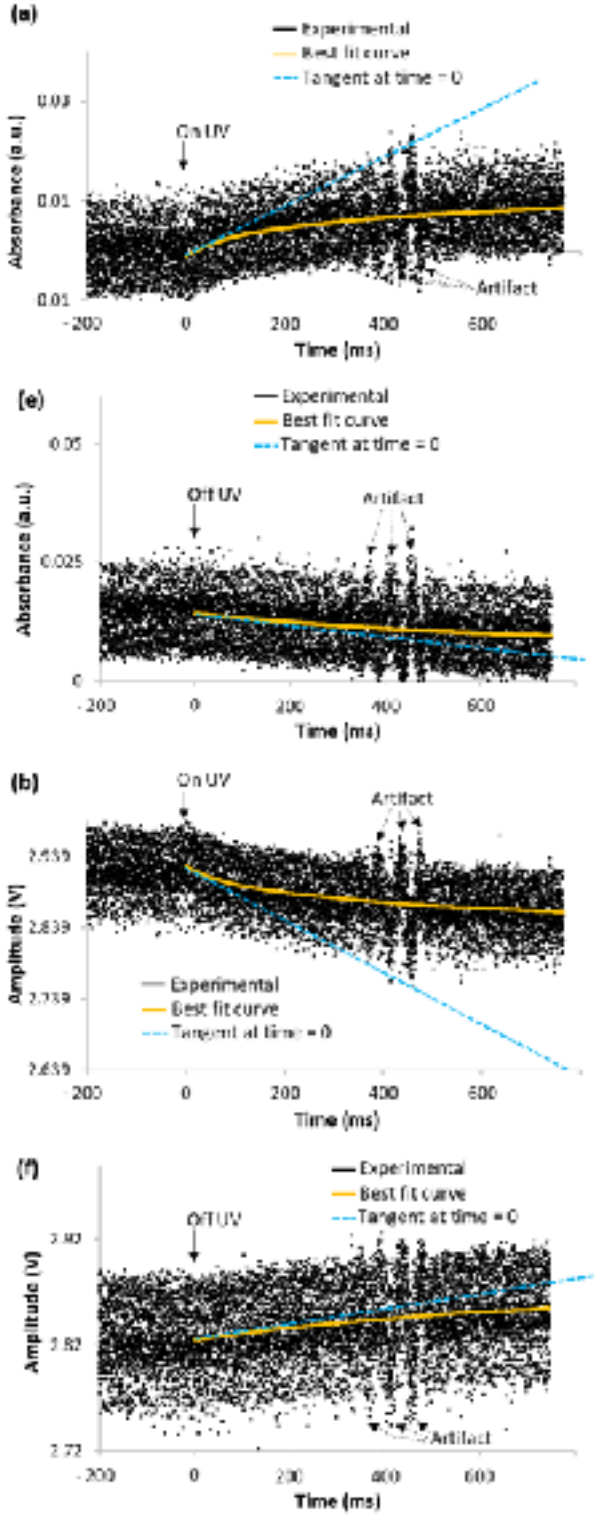

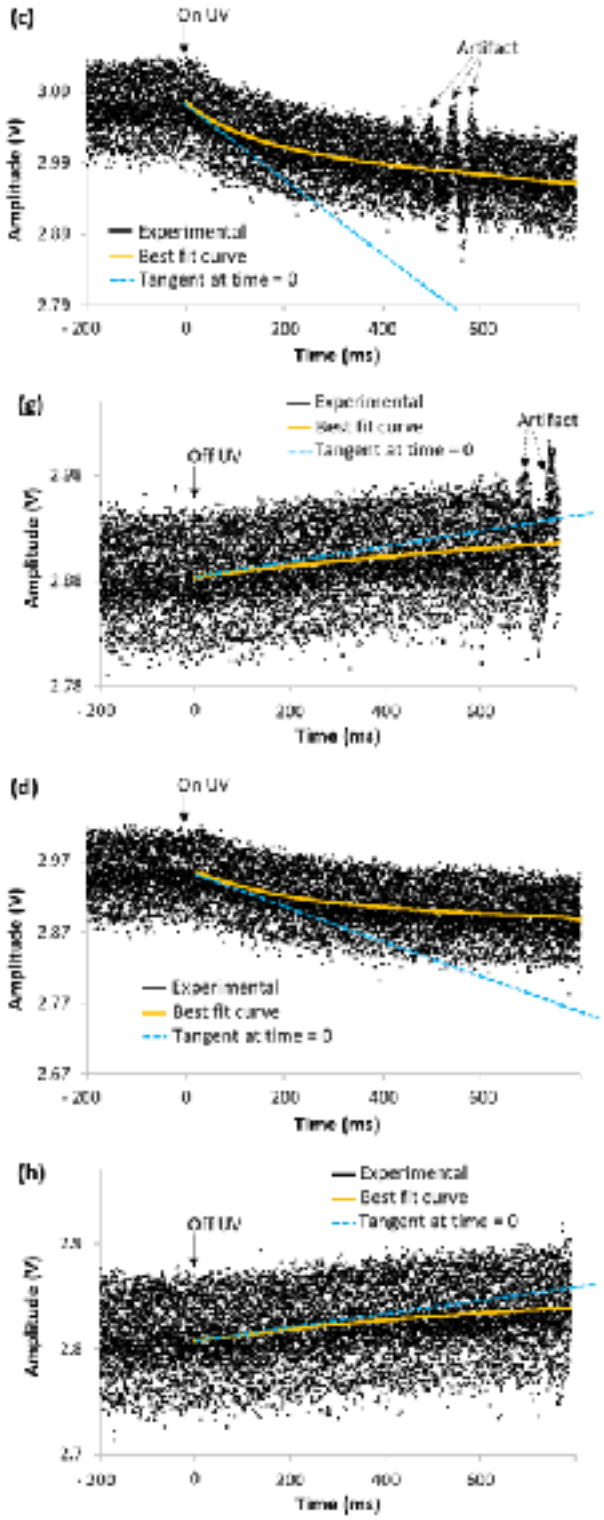

Figure S7. QCL signal at 1360 cm^{-1} *vs* time over TiO_2 HA during repeated UV on-off cycles (UV on: a-b-c-d, UV off: e-f-g-h; two panels on the same horizontal line forming one UV on-off cycle) under reaction flow at 25 °C and atmospheric pressure. (a) and (e) show the same UV on-off cycle as (b) and (f), but with a y axis expressed in absorbance instead of amplitude. Conditions: flow = 30 mL/min; 0.1 and 20 vol.% of methanol and oxygen in argon, respectively; Hg-Xe lamp (200 W); $I_0 \approx 200$ mW/cm^2. In (a-b-c-d), time = 0 corresponds to the moment when the shutter in-between the lamp and the UV-light guide directed to the IR cell was opened to irradiate the sample. During the preceding 200 ms, the sample was already under reaction flow but still in the dark. In (e-f-g-h), time = 0 corresponds to the moment when the shutter was closed again, still under reaction flow. The times to open and close the shutter were around 6.5 ms and 3.2 ms, respectively.

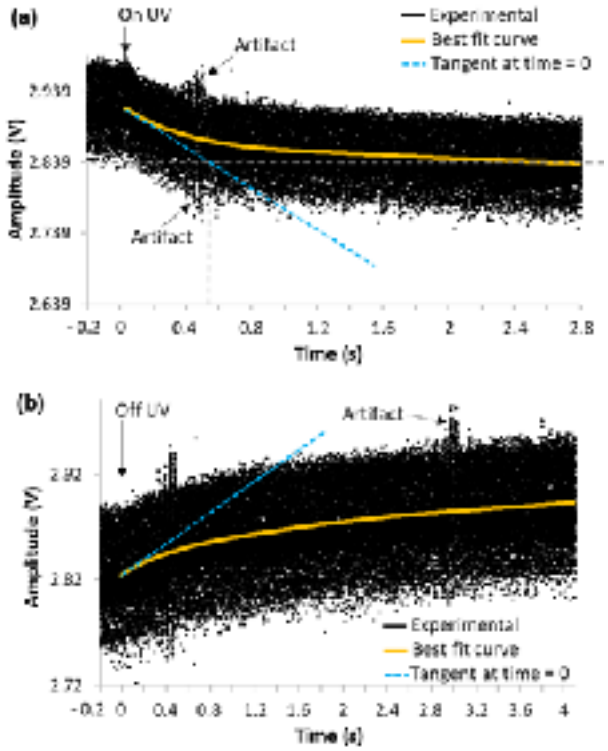

Figure S8. Same UV on(a)-off(b) cycle as shown on Figure S7 (b and f, respectively), but over a longer time scale.

- **QCL beam absorbance at 1360 cm^{-1} *vs* time over TiO_2 P25 under reaction flow at 25 °C, in the UV off period following an UV on period of 300 ms *vs* 5 s.**

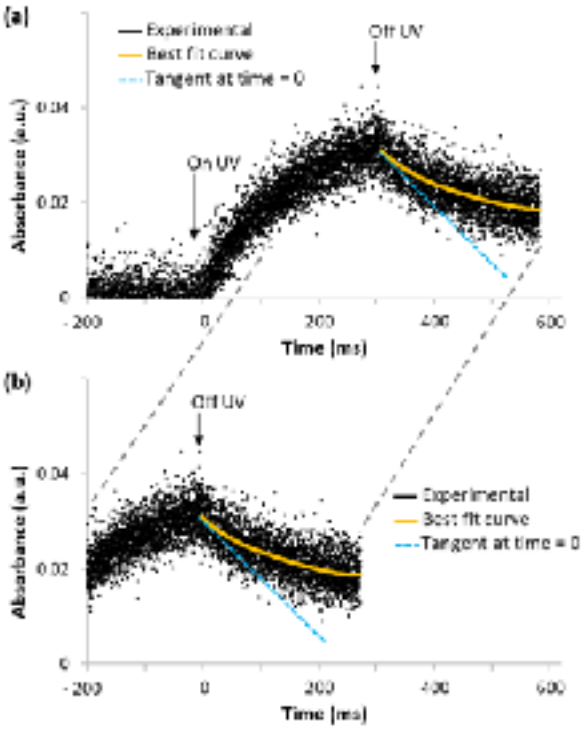

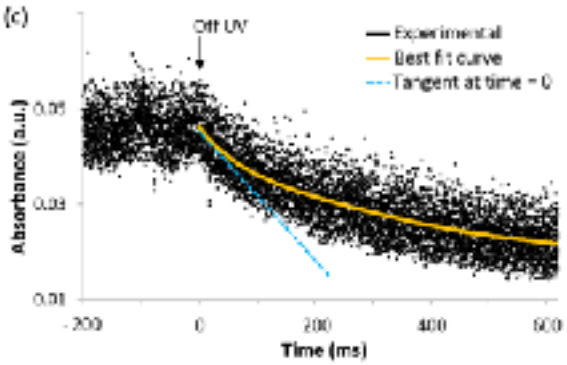

Figure S9. QCL beam absorbance at 1360 cm^{-1} *vs* time over TiO_2 P25 under reaction flow at 25 °C and atmospheric pressure during (a-b) a UV on-off cycle with on and off periods of 300 ms and (c) the same UV off cycle as shown on Figure S3e, i.e. after a UV on period of 5 s. Conditions: flow = 30 mL/min; 0.1 and 20 vol.% of methanol and oxygen in argon, respectively; Hg-Xe lamp (200 W); $I_0 \approx 200$ mW/cm². In (a), time = 0 corresponds to the moment when the shutter in-between the lamp and the UV-light guide directed to the IR cell was opened to irradiate the sample. During the preceding 200 ms, the sample was already under reaction flow but still in the dark. In (b-c), time = 0 corresponds to the moment when the shutter was closed again, still under reaction flow. The times to open and close the shutter were around 6.5 ms and 3.2 ms, respectively. Extracted $R_{app,r}$ values are 0.12 in (b) *vs* 0.15 in (c).

- **QCL beam absorbance at 1360 and 1310 cm^{-1} *vs* time over TiO_2 P25 getting UV-irradiated under flowing methanol at 25 °C in the absence *vs* presence of oxygen.**

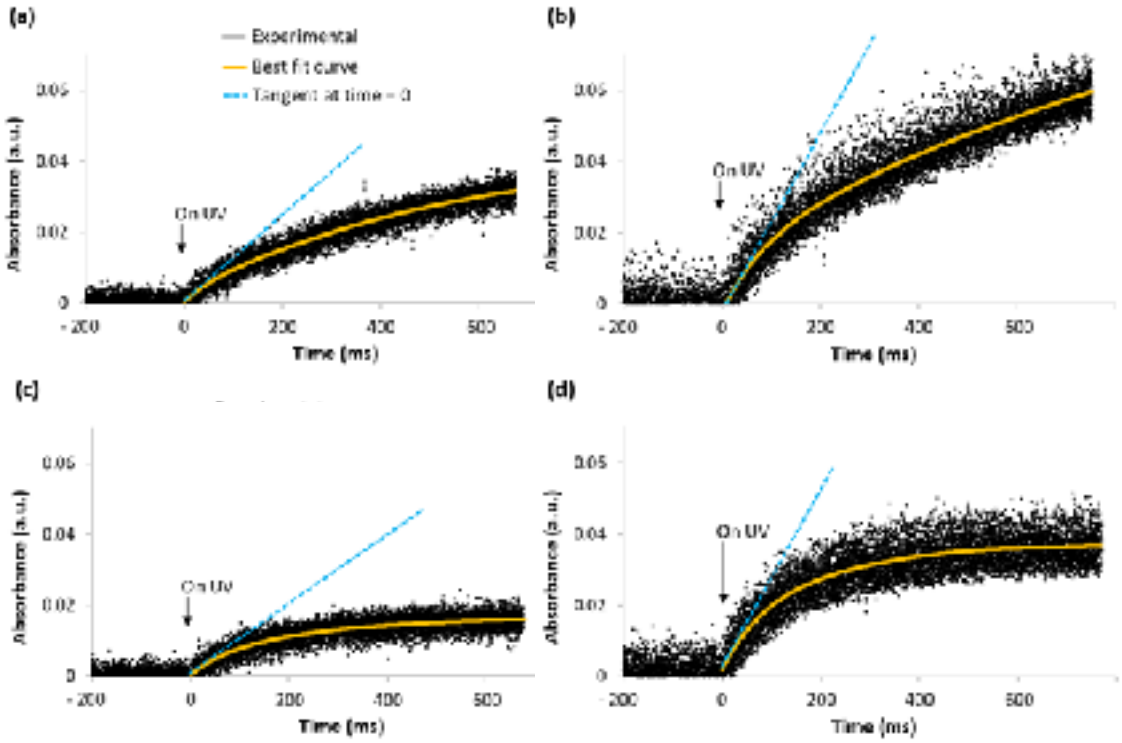

Figure S10. QCL beam absorbance at 1310 cm^{-1} (a and c) and 1360 cm^{-1} (b and d) *vs* time over TiO_2 P25 getting UV-irradiated under flowing methanol at 25 °C and atmospheric pressure in the absence (a-b) or presence (c-d) of oxygen. Conditions: flow = 30 mL/min; 0.1 vol.% of methanol in argon, with 20 vol.% of oxygen if present; Hg-Xe lamp (200 W); $I_0 \approx 200$ mW/cm². Time = 0 corresponds to the moment when the shutter in-between the lamp and the UV-light guide directed to the IR cell was opened to irradiate the sample. During the preceding 200 ms, the sample was already under flowing methanol (without oxygen in a-b, with oxygen in c-d) but still in the dark. The time to open the shutter was around 6.5 ms.